Ab initio study of cubyl chains and networks

F. Valencia and A. H. Romero
Advanced Materials Department, IPICyT, Camino a la Presa San José, 2055 Colonia Lomas 4ta. sección, San Luis Potosí (SLP), Mexico

Miguel Kiwi and R. Ramírez
Facultad de Física, Pontificia Universidad Católica de Chile, Casilla 306, Santiago 6904411, Chile

A. Toro-Labbe
Facultad de Química, Pontificia Universidad Católica de Chile, Casilla 306, Santiago 6904411, Chile

(Received 1 July 2004; accepted 19 August 2004)

The spatial arrangements and physical properties of one- and two-dimensional structures, based on the amazing cubane (C_8H_8) molecule, are investigated in detail. In particular, we compute the electronic structure, both by first principle calculations and by semiempirical methods. The elastic and vibrational properties are evaluated as well. All these results are compared with those of the single cubane molecule, in order to elucidate the influence of dimensionality. © *2004 American Institute of Physics.* [DOI: 10.1063/1.1805492]

I. INTRODUCTION

Since the discovery of the perfect cubic structure of cubane: C_8H_8, an important effort has been carried out to understand the amazing properties of this molecule.[1] May be the most remarkable characteristic of this hydrocarbon allotrope is the 90° angle of the C–C–C bond, far from the diamond sp^3 hybridization angle, which is 109.5°. This molecular strain has important consequences on the heat of formation (+144 kcal/mol) and other energetic properties. In spite of this fact, the synthesis of this molecule was achieved by Eaton and Cole[1] with a rhombohedral molecular crystal structure. In addition, cubanes are considered as one of the most promising compounds for use in the explosive and propellant industries.[2]

The single molecule and its crystalline form have been characterized by different means both experimentally[1,3–10] and theoretically.[11–16] Both approaches indicate that the molecule and the crystal are very stable at room, and even higher, temperatures; moreover, its peculiarities are dominated by those of the cubane molecule. At present a first principle study of the physicochemical properties of linear and surfacelike cubane oligomers, as a function of monomer number, is well advanced and will be published elsewhere.[10] On the other hand, their synthesis path has been taken even further, since Eaton *et al.* found a way to create polycubanes.[9,17] First they obtained cubylcubane by nucleophilic additions of cubene (1,2-dehydrocubane).[17] Later on they developed an experimental path to obtain *p*-[*n*] cubyls and aryl-substituted cubanes, opening the possibility of creating, in a very controlled fashion, polycubanes[9] as one- and two-dimensional polymers.

In this contribution we report first principle results, as well as semiempirical calculations (similar to those implemented by Rurali and Hernández[18]), with a tight-binding parametrization as in Ref. 19, carried out both for hypothetical one-dimensional chains and two-dimensional polycubane networks. In fact, similar one-dimensional structures built using cubene (dehydrogenated cubane) units have been proposed previously as small gap polymers.[20] Here we focus on hydrogen saturated chains following a path that stays closer to experiment. As discussed in the Appendices, there perfectly periodic models do describe the actual behavior of finite size (Appendix A) and bent (Appendix B) oligomeric chains with acceptable accuracy. Elastic, electronic, and vibrational properties are calculated and compared to those of the single cubane molecule, in order to determine the influence of dimensionality. Calculations were performed within density functional theory framework, using a plane wave basis set and a pseudopotential approach.[21] The code we used was the PWSCF (plane waves self-consistent field) of Baroni *et al.*[21] The pseudopotentials employed were of the ultrasoft/Vanderbilt kind,[22] and the exchange correlation term was treated with the Perdew-Wang[23] scheme. Kinetic energy cutoffs of 20 Ry for the wave functions, and 120 Ry for the charge densities and potentials, were used throughout. Convergence on *k* points and energy cutoff were performed and here we only present the converged results. In the tight-binding calculations we have compared geometries and electronic properties by using as input the optimized results from the *ab initio* calculation. The cubane molecule retains its structure, since the electronic properties are close to the *ab initio* results.

II. GEOMETRY AND ENERGETICS

First we performed a Broyden-Fletcher-Goldfarb-Shanno (BFGS) (Ref. 24) relaxation of a single cubane molecule (Fig. 1). We embedded the single molecule in a cubic box with sides 11.64 Å long, which corresponds to more than five times the molecule size, to avoid interactions with periodic images. The geometry obtained was quite consistent with the experimental data[1,4] and other theoretical calculations.[16] In fact, C–C distances of 1.571 Å, C-H distances of 1.098 Å, C–C–H angles of 125.3° and C–C–C angles of 90.0° were found. Although symmetry was not

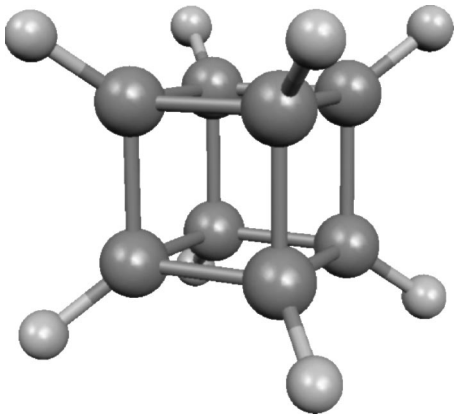

FIG. 1. The cubane C_8H_8 molecule.

imposed during relaxation we have found only small deviations from the full cubic symmetry, reflected by tiny variations around the mean for the angles and distances (0.0002 Å for the C–C distance, 0.015° for the C–C–C bond and 0.1° for the C–C–H bond). As will be discussed below, these small deviations induce only minor artificial unfolding of electronic and vibrational states. Thus, we conclude that the level of theory used is quite sufficient to describe these cubanecubyl systems.

Next we consider three different kinds of infinite cubyl rod cubanes, as depicted in the insets of Fig. 2. Each model consists a covalently bonded chain, which is constructed as a periodic repetition of the finite oligomeric cubyl rods experimentally realized by Eaton *et al.*[9] Model (a) consists of cubylcubane blocks joined along the cube diagonal, which is also the chain axis; model (b) is a stairlike structure with the chain axes parallel to one of the cubyl faces; and model (c) is similar to model (a), but in the staggered C–H bond configuration. Relaxation of the internal coordinates and the lattice parameter (c_0) of the cubyl chains was performed using eight special k points for models (a) and (c) and four for model (b). Tetragonal simulation boxes were used. The lattice vectors of the tetragonal cell are $\vec{a}=a\hat{x}$, $\vec{b}=a\hat{y}$, and $\vec{c}=c\hat{z}$, where $(\hat{x},\hat{y},\hat{z})$ form an orthogonal basis and $\hat{z}$ is the growth direction. The ratios between the sides of the simulation box that we adopted are $c/a=0.25$ for models (a) and (c) and $c/a=0.5$ for model (b), in order to avoid interactions with periodic images along the xy plane. As can be seen from Fig. 2, model (c) lies in a very unstable site of the potential energy surface and the BFGS relaxation pushes it towards the eclipsed model (a) configuration, which is stable, in agreement with previous calculations on cubylcubane.[14] For structures (a) and (b) the binding energies ($E_b=E_{chain}-E_{atoms}$) per cubyl unit are basically the same (89.6 eV), which means that the binding energy is mainly determined by the the intercubyl bond arrangement rather than by the detailed geometry of the building blocks.

Model (a) has a stable minimum for $c_0=4.20$ Å. The shared carbon atoms are pulled towards each other, so that the six cage bonds at α positions are longer than those far apart from these intercage bonds (1.581 Å against 1.567 Å). The intercubyl bond is significantly shorter: 1.462 Å and it makes an angle of 125.6° with the cubyl edges. Inner bond angles are also affected by the setting of the intercubyl bond: a shift of the α-positioned bonds towards 89.5° is observed, accompanied by a shift of the opposite angle on the same cube face towards 90.5°, while the remaining bond angles stay put very close to 90°. The same kind of cubyl stretching was predicted to happen in cubane oligomers.[10] On the other hand, neither C-H distances nor C-C-H bond angles are af-

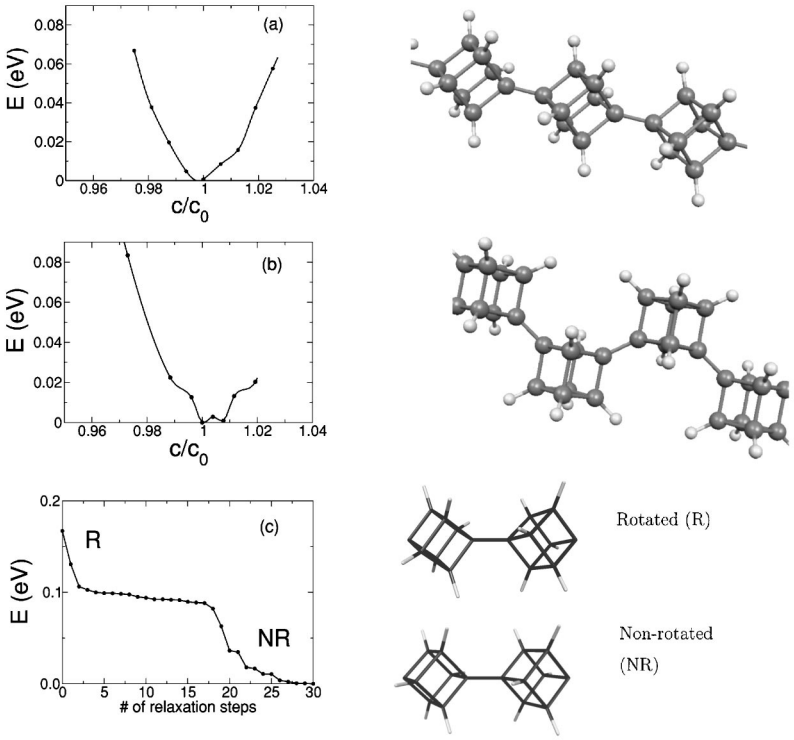

FIG. 2. Energetics and geometries for the one dimensional chain models. In all the above figures the zero energy level corresponds to the total minimal energy. (a) Energy vs axial deformation for the cubyl-cubane chain illustrated on the right; (b) energy vs axial deformation for the cubyl-cubane ladder structure illustrated on the right; (c) energy relaxation path for the transition between successive rotated and non-rotated cubanes, as illustrated on the right side.

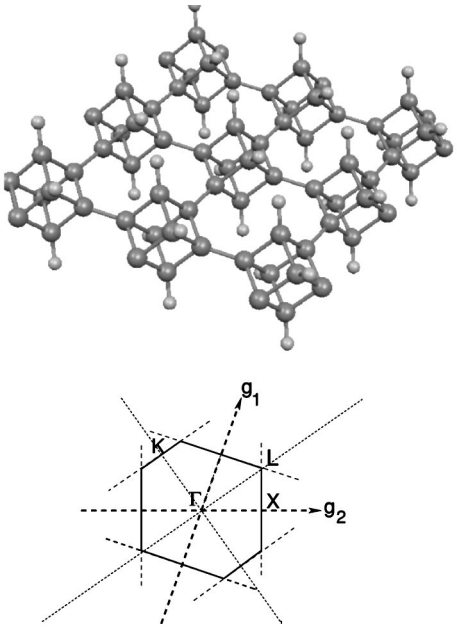

FIG. 3. A two-dimensional cubyl network with its corresponding Brillouin zone.

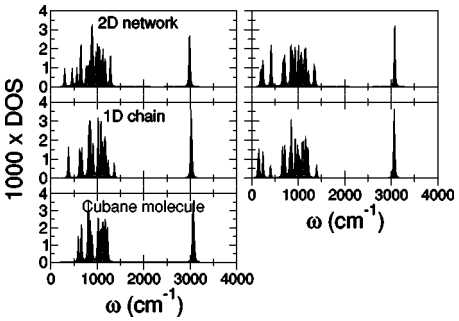

FIG. 4. Vibrational density of states (DOS). The left hand graphs correspond to the Γ point for the 2D cubane network (top), the 1D cubane chain (middle), and the cubane molecule (bottom). The right hand plots correspond to spectra at the *X* point.

fected and their values remain the same as in the molecular case, a behavior expected because of the large separation between C-H pairs belonging to different cubyl units. To obtain an idea of the mechanical strength one can define a longitudinal elastic constant in the usual way, i.e. via the curvature of the energy plot at the equilibrium position: $K=(d^2E/d\zeta^2)$, where $\zeta=c/c_0$ is the lattice deformation parameter in the axial direction, which yields a value of $K=191$ eV. If we were to build an array of aligned rods, this elastic constant would yield a Young's modulus of around 200–400 GPa in the axial direction.

For model (b) $c_0=6.85$ Å, the intercubyl bond is 1.471 Å and makes an angle of 125.6° with the cubyl edges, just as in model (a). The intercage bonds on the α position are 1.580 Å long, while those far from the intercage bond, which lie perpendicular to the chain axis, are 1.567 Å long and those lying parallel to the axis are 1.569 Å long. Again, the bond angles centered at shared carbons are shifted to 89.5°, a shift that is compensated by rearrangement of the remaining angles, which remain close to 90°. Because of the shape of the energy vs c_0 plot near the optimal value, an elastic constant defined as in the previous case would not make much sense. It is also interesting to stress the correspondence between the bond lengths in this infinite chain and those calculated for stairlike oligomers.[10]

Finally, we consider a two-dimensional cubyl network as shown in Fig. 3: the primitive vectors lie parallel to the cube diagonals, which define a two-dimensional (2D) oblique lattice. Our calculation has been defined by using the 2D Brillouin zone illustrated in Fig. 3. The third axis, perpendicular to the cubyl network, has been set to be three times larger than the axis of the bidimensional network to avoid interaction with periodic images. Once again, we performed the relaxation procedure for the internal coordinates and lattice parameters and the optimal lattice parameter is $a_0=4.23$ Å. A geometry with four different C-C bond lengths: 1.449 Å for the intercage bonds, 1.60 Å for the cubyl bond at α position with two intercage bonds, 1.579 Å for bonds at α position with one single intercage bond, and 1.555 Å for bonds far from the intercage bond, was obtained. In contrast with the 1D cases, the C-H bonds are now slightly affected by the network setup; the C-H distances are slightly compressed to 1.097 Å and the C-C-H angles become distorted: when the C-C bond includes one of the shared carbon atoms the C-C-H angle is 124.0°, and 125.1° otherwise. Distortion of the inner cubyl angles is also larger than in the 1D chains: angles including a bond far from the intercage bond shift to 90.8° and the opposite angles consequently shift to 89.2°. The positive curvature of the energy as a function of the area is indicative of the 2D network stability. Defining now an elastic constant using the curvature of the energy vs area plot: $K'=(d^2E/d\sigma^2)$, where $\sigma=a/a_0$, we obtained $K'=108$ eV, which is related to the energy delivered by the system when the network is subject to an isotropic deformation along the unit cell vectors. Under orthorombic deformations of the lattice vectors it is observed that the energy is well fitted by a quadratic function $E=E_o+1/Cz^2$, where the deformation parameter is related to the ratio between the lengths of the basis vectors in the plane: $z=1-(a/c)$ and the constant $C=74.38$ eV, thus showing that the system is stable under this nonisometric tensions.

It is clear that the cubyl blocks, both in 1D chains and 2D networks, remain very close to the molecular geometry with small deformations related to the setup of intercubyl chains. Thus, the stability of the whole network is related to the molecular stability and the strong intercage bond.

III. VIBRATIONAL SPECTRA

We calculated the vibration frequencies for a single cubane molecule and found differences of 5% with previous calculations[16] and also with experimental measurements.[8] This stresses the reliability of our calculations, which we now extend to properties of 1D and 2D networks. For the 1D case we have limited our attention to model (a). The calculated vibrational spectra (Γ- and *X*-point vibrations) are reported in Fig. 4, both for the cubane molecule and the 1D and 2D cubane networks. Even though we have considered a large box, some interaction between images lead to the ap-

pearance of spurious modes which are not included in our results, since they correspond to pure rotations or pure translations of the whole system. All our frequencies (at Γ and X) are positive, which constitutes another indication of the mechanical stability of the whole system.

In the case of the single cubane molecule (left bottom in Fig. 4), deviations from the full O_h symmetry (molecular symmetry) leads to the splitting of the expected 18 modes[8,16] of the cubane molecule into 42 different frequencies. However, the vibrational modes displayed at the bottom of Fig. 4 are well within the accuracy of previous theoretical and experimental results.[8,16] The molecular breathing mode lies at 1008 cm^{-1} in the present calculation and around 947.4 cm^{-1} in the HF/6-31G calculations of Ref. 8. The two peaks around 600 cm^{-1} and 650 cm^{-1} correspond to C-C-C bending modes, while the peaks around 800 cm^{-1}, 850 cm^{-1} and 900 cm^{-1} correspond to stretching modes of the C-C bonds; following the 1008 cm^{-1} breathing mode, there is another C-C-C bending mode and C-C-H bending modes up to 1222 cm^{-1}. The C-H stretching mode is quite sharp and appears around 3000 cm^{-1}. It is characteristic of the cubane molecule and persists in the chains and two-dimensional structures. This assignment is consistent with that of Ref. 16.

The lowest lying modes of the cubane chain lie around 380 cm^{-1} and are coupled, in phase, rigid rotations around an axis perpendicular to the chain axis of the cubylcubane units. Breathing modes are no longer present because they are hindered by the intercage bond. There is also a blueshift of the C-C-C bending, C-C stretching, and C-C-H bending modes and a redshift of the C-H stretching modes. Another well-defined peak lies around 1367 cm^{-1}, due to strong vibrations of the carbon atoms along the chain axis (cube diagonal). The C-H stretching modes are slightly redshifted.

In the two-dimensional network coupled rotation modes, around two axis in the plane and one perpendicular to the network, arise around 299 cm^{-1}, 460 cm^{-1}, and 560 cm^{-1}, respectively (left top in Fig. 4). Again there is a peak associated with strong atomic motions along the network axes (cube diagonals) which lies around 1278 cm^{-1}. There are also some C-C stretching modes shifted to the 900 cm^{-1} region, and some C-C-H bending modes shifted to the 1000 cm^{-1} region increasing the vibrational density of states (DOS) between 900–1000 cm^{-1}. Again the C-H stretching modes are redshifted.

In order to study the vibrational dispersion we have also calculated the vibrational DOS at the X point, as illustrated on the right-hand side of Fig. 4. The high energy modes (corresponding to optical modes) have little dispersion, as was expected from the strong molecular character of these C-H stretching modes, and they could be represented by an single Einstein mode. Instead, the acoustic modes change radically, both in the 1D and in the 2D case, as expected from their collective character. In what follows we will describe some of the major changes observed. The X-point (counterphase) coupled rotations appear at 136 cm^{-1}, 152 cm^{-1}, and 159 cm^{-1} in the 1D case, and at 193 cm^{-1}, 414 cm^{-1}, and 415 cm^{-1} for the 2D network. Counterphase displacements of cubyl units in a direction perpendicular to the chain axes lead to a 245 cm^{-1} mode for the 1D chain,

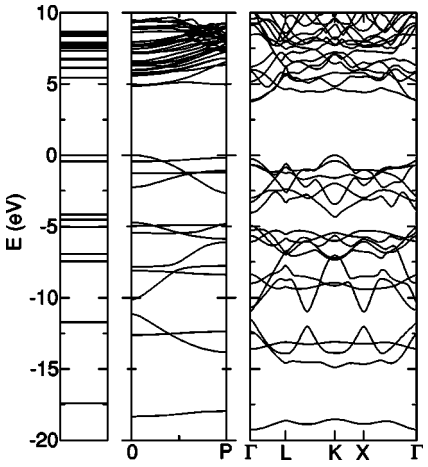

FIG. 5. Electronic band structure for cubyl chain (middle panel) and network (right panel) compared to the electronic levels of the cubane molecule (left panel). The special points in the first Brillouin zone of the two-dimensional network are depicted in Fig. 3. $E=0$ always corresponds to the highest occupied energy level.

and two modes at 234 cm^{-1} (out of plane vibrations) and 246 cm^{-1} (in plane vibrations) for the 2D network. Finally, very energetic modes, involving the stretching of the intercage bonds, appear near 1350 cm^{-1} in both cases.

IV. ELECTRONIC SPECTRA

The electronic band structures of the different cubane systems are shown in Fig. 5, and the corresponding DOS for the lowest energy configuration in Fig. 6. In Fig. 5 the band structure of the different cubane networks is compared with the electronic levels of the cubane molecule. As expected, there is a clearcut energy shift of the HOMO-LUMO (highest occupied molecular orbital–Lowest-unoccupied molecular orbital), from 5.43 eV for the cubane molecule to a 4.87 eV gap for the 1D cubyl chain and a 3.78 eV gap for the 2D network, which is an indication that dimensionality contributes to the electronic delocalization. Also, the increase in the band structure curvature as function of dimensionality is clearly noticeable, which implies a decrease of the effective electron mass, especially close to the Fermi level. The lower electronic level retains its molecular character, as can be seen from the very low dispersion of the band structure. This is

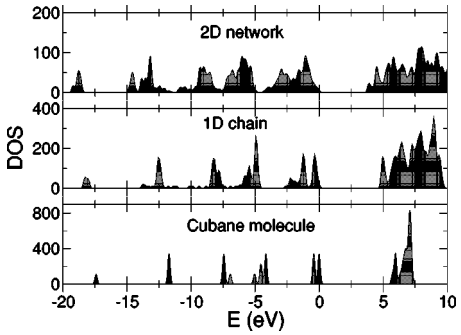

FIG. 6. Electronic density of states for the cubane molecule (bottom), the cubyl chain (middle) and the cubyl 2D network (top). The zero level in each case is the highest occupied energy (HOMO) level.

also true for other electronic bands, as can be seen in Figs. 5 and 6, in particular for the first virtual modes of the one-dimensional chain. This means that conduction would be rather difficult, even promoting electrons across the large band gap (for the sake of comparison: the calculated value for diamond in the same theory level is about 4.1 eV). In the two-dimensional network we have an indirect gap and a larger dispersion at the Γ point for the first virtual electronic states. We find much more valence states available near the Fermi energy, which increases the surrounding density of states as can be seen in the band structure and DOS figures. Inclusion of dopants or functional groups within the chain and/or network could lead to semiconductor character, and even to metallic behavior, according to our calculations.[25]

V. CONCLUSIONS

We have studied, by first principle calculations, the geometric, electronic and vibrational properties of 1D and 2D cubanes networks. The cubane molecule is well described by the level of our theory and our agreement for the various physical properties is quite satisfactory. As the dimensionality is increased the electronic properties change by decreasing the electronic gap and creating more valence states close to each other. The dispersion is also increased by dimensionality. The optimal geometry obtained from our calculation predicts a network where the basic building block corresponds to a slight distortion of the single cubane molecule. The lowest energy configuration of the 1D network corresponds to a series of cubanes in an staggered configuration. In the 2D case the network forms an oblique lattice, with a lattice parameter similar to the 1D case. The vibrational properties also change with dimensionality, but with little dispersion for the highest energy modes, which correspond to molecular C-H stretching. As the dimensionality increases low energy acoustic modes set in, which have a large dispersion as revealed by our X-point vibrational DOS.

All in all, we have investigated the spatial arrangements and physical properties of one- and two-dimensional structures of the amazing cubane (C_8H_8) molecule. In particular, the electronic characteristics, obtained both by first principle calculations and semiempirical methods, as well as the elastic and vibrational properties, were compared with those of the single cubane molecule to asses the influence of dimensionality. This way we have found a system with very interesting elastic qualities (Young's modulus higher than 200 GPa) but which maintains the molecular electronic properties that correspond to an insulator. Moreover, it has rather flat optical phonon bands and an acoustic branch that should exhibit strong electron-phonon coupling. We hope that these predicted properties will be investigated experimentally, in particular the mechanical stability and electronic behavior, to determine if these oligomeric systems are of interest in the development of electronic nanodevices.

ACKNOWLEDGMENTS

The authors acknowledge the computer time allocation on the Cray T3E at the Centro Nacional de Supercomputo-IPICyT. F.V. acknowledges a Ph.D. scholarship from IPICyT. M.K., R.R., and A.T.L. were supported by FONDECYT under Grant Nos. 1030957, 1040356, and 1020534, respectively. M.K. and R.R. also acknowledge support by Fundación Andes. A.H.R. is thankful for the support of CONACYT-Mexico under Grant No. J-42647-F.

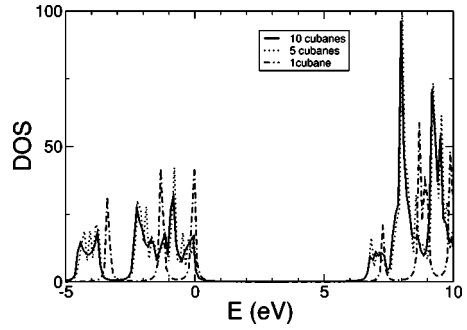

FIG. 7. Electronic density of states (DOS) for finite oligomeric chains, calculated within a tight binding approach. Continuous line: chain of 10 cubyl cubane units; dotted line: 5 cubyl cubane units; dashed line: one single cubane molecule. The small changes between the 5 and 10 cell cases imply that these oligomeric chains already closely approach the 1D crystalline behavior. The zero energy level always is the highest occupied energy level.

APPENDIX A: FINITE SIZE EFFECTS

Perfect periodicity is, of course, only an approximation to treat a real problem of a rather large number of atoms. But, it simplifies the problem both conceptually and computationally and yields, more often than not, qualitatively correct results. However, it is important to check the validity of this approximation for reasonably small (real) oligomers. Thus, we performed tight binding calculations using the Pettifor parametrization for hydrocarbons[19] on a series of finite, hydrogen saturated, oligomeric chains constructed on the basis of the relaxed building block of model (a). This tight binding approach allows us to treat a larger number of cubyl units retaining an adequate description of the electronic properties. The evolution of these properties, as the number of cubyl units increases (see Fig. 7), clearly shows that the electronic properties reach the crystalline limit after a rather small size is reached, which in our case amounts to just five cubane cubyl units.

APPENDIX B: EFFECTS DUE TO CUBYL CUBANE CHAIN BENDING

Throughout this contribution we assumed that oligomeric chains are built following a straight line. Now we consider the effects related to the bending of finite oligomeric chains, like the ones already discussed in Appendix A. For this purpose we have altered the finite chains by rotating each cubyl unit by an angle ϕ with respect to the previous one, while preserving the cubyl geometries and intercage bond lengths. Energetic and electronic properties of this altered chains were studied within the same tight-binding approach of Appendix A. In all these cases the strain energy associated with this kind of bending increases quadratically with the bending angle ϕ, so that the associated elastic constants $K_{bend}=1/2(d^2E^{cu}_{strain}/d\phi^2)$ where E^{cu}_{strain} is the strain energy per cubyl cubane unit, are always positive (see the

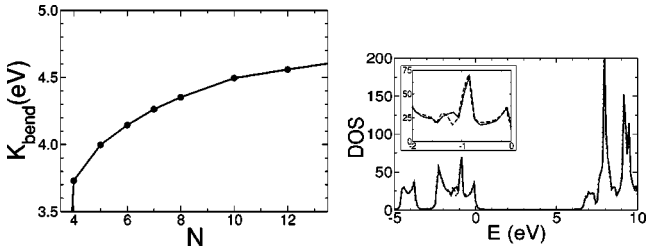

FIG. 8. Effect of the chain deflection on the energy and electronic properties of finite oligomers. Left panel: elastic stiffness against bending, as function of the number of cubane units. Right panel: electronic DOS for a 14 unit oligomer before and after bending; the continuous line corresponds to the straight rod, and the dashed line to the bent rod. The inset corresponds to the only energy interval ($-2 \leqslant E \leqslant 0$ eV) where the bent and straight rod DOS differ significantly.

left plot of Fig. 8). It is also interesting to notice that the electronic DOS is only slightly sensitive to the chain curvature, as seen on the right side of Fig. 8.

[1] P. E. Eaton and T. W. Cole, Jr., J. Am. Chem. Soc. **86**, 3158 (1964).
[2] P. E. Eaton, R. L. Gilardi, and M.-X. Zhang, Adv. Mater. (Weinheim, Ger.) **12**, 1143 (2000).
[3] A. S. Pine, A. G. Maki, A. G. Robiette, B. J. Krohn, J. J. G. Watson, and T. Urbanek, J. Am. Chem. Soc. **106**, 891 (1984).
[4] E. B. Fleischer, J. Am. Chem. Soc. **86**, 3889 (1964).
[5] J. C. Facelli, A. M. Orendt, M. S. Solum, G. Depke, D. M. Grant, and J. Michl, J. Am. Chem. Soc. **108**, 4268 (1986).
[6] T. Yildirim, P. M. Gehring, D. A. Neumann, P. E. Eaton, and T. Emrick, Phys. Rev. Lett. **78**, 4938 (1997).
[7] T. Yildirim, P. M. Gehring, D. A. Neumann, P. E. Eaton, and T. Emrick, Phys. Rev. B **60**, 314 (1999).
[8] T. Yildirim, Ç. Kiliç, S. Ciraci, P. M. Gehring, D. A. Neumann, P. E. Eaton, and T. Emrick, Chem. Phys. Lett. **309**, 234 (1999).
[9] P. E. Eaton, K. Pramod, T. Emrick, and R. Gilardi, J. Am. Chem. Soc. **121**, 4111 (1999).
[10] B. Herrera, F. Valencia, A. H. Romero, M. Kiwi, R. Ramírez, and A. Toro-Labbé (unpublished).
[11] S. L. Richardson and J. L Martins, Phys. Rev. B **58**, 15307 (1998).
[12] C. A. Scamehorn, S. N. M. Hermiller, and R. M. Pitzar, J. Chem. Phys. **84**, 833 (1986).
[13] J. Almlof and T. Jonvik, Chem. Phys. Lett. **92**, 267 (1982).
[14] B. Herrera and A. Toro-Labbé, Chem. Phys. Lett. **344**, 193 (2001).
[15] T. Yildirim, S. Ciraci, Ç. Kiliç, and A. Buldum, Phys. Rev. B **62**, 7625 (2000).
[16] K. Miaskiewicz and D. A. Smith, Chem. Phys. Lett. **270**, 376 (1999).
[17] P. E. Eaton, Angew. Chem. **31**, 1421 (1992).
[18] R. Rurali and E. Hernández, Comput. Mater. Sci. **28**, 85 (2003).
[19] A. P. Horsfield, P. D. Godwin, D. G. Pettifor, and P. Sutton, Phys. Rev. B **54**, 15773 (1996).
[20] P. M. V. B. Barone, A. Camilo, Jr., and D. S. Galvão, Synth. Met. **102**, 1410 (1999).
[21] S. Baroni, A. Dal Corso, S. de Gironcoli and P. Giannozzi, http://www.pwscf.org
[22] D. Vanderbilt, Phys. Rev. B **41**, 7892 (1991).
[23] J. P. Perdew, J. A. Chevari, S. H. Vosko, K. A. Jackson, M. R. Pederson, D. J. Singh, and F. Carlos, Phys. Rev. B **46**, 6671 (1992).
[24] D. F. Shanno, Math. Comput. **24**, 647 (1970), See also the summary in: D. F. Shanno, J. Optim. Theory Appl. **46**, 87 (1985).
[25] F. Valencia, A. H. Romero, M. Kiwi, R. Ramírez, and A. Toro-Labbé (unpublished).